INTERNATIONAL JOURNAL OF HYDROGEN ENERGY XXX (2015) 1–11

Available online at www.sciencedirect.com

ScienceDirect

journal homepage: www.elsevier.com/locate/he

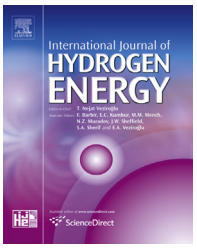

A DFT study of hydrogen storage in $Zr(Cr_{0.5}Ni_{0.5})_2$ Laves phase

A. Robina Merlino [a,b], C.R. Luna [b], A. Juan [b,*], M.E. Pronsato [b]

[a] Facultad de Ingeniería, Universidad Nacional de la Patagonia San Juan Bosco, Ciudad Universitaria, 9005 Comodoro Rivadavia, Chubut, Argentina

[b] Departamento de Física & IFISUR (UNS–CONICET), Universidad Nacional del Sur, Av. Alem 1253, B8000CPB, Bahía Blanca, Buenos Aires, Argentina

ARTICLE INFO

Article history:
Received 29 September 2015
Received in revised form
21 October 2015
Accepted 22 October 2015
Available online xxx

Keywords:
C14 Laves phase
Hydrogen absorption
Ab initio
Bonding
Metal–hydrogen bond

ABSTRACT

Theoretical studies on the total energy, electronic structure and bond of $Zr(Cr_{0.5}Ni_{0.5})_2$ intermetallic compound and its hydrides were performed using density functional calculations. The optimized *c/a* ratio was found in good agreement with experimental data of the C14 Laves phase. When hydrogen is introduced in the AB_2 matrix (A = Zr; B = Ni, Cr) the A_2B_2 sites are preferentially occupied in the structure, followed by the AB_3 while B_4 remains empty. The volume of the intermetallic increases up to 52.19% when 28H are absorbed in the unit cell, whereas the binding energy remains practically the same up to −6.76 eV/H, indicating little interaction. Among hydrogenations the main contribution to density of states is due to *d* electrons of all components of the structure. H-metal bonding is detected in the range −8 to −6 eV. Above 8H the magnetic moment increases with respect to the pure Laves phase.

Introduction

It is well known the interest to find renewable, sustainable and cleaner energy sources to replace the fossil fuels. The fossil fuel-based energy causes a significant environmental impact and it is the subject of a strong economic and geopolitical discussion [1]. One possible technical way to overcome these issues is the hydrogen-based economy [2–4]. The hydrogen vector is considered the most promising energy carrier due to its potentially abundant production from clean sources. Nevertheless, apart from hydrogen production costs, there are some drawbacks related to its very low density, i.e. hydrogen storage and carrying.

Solid state hydrogen storage materials, like reversible AB intermetallic compound, are currently an area of intense research [5–7]. Particularly, the AB_2 or Laves phases, have been extensively studied due to their hydrogen high storage capacity, good hydrogen absorption/desorption kinetics and cycle life, among others [8,9]. The A metal can be Mg, Zr, or Ti while the B metal can be Ni, V, Cr, or Mn [10]. It was proved that the compositional substitutions of metallic elements in Zr-based AB_2 Laves structures, such as $ZrMn_2$, $ZrCr_2$ and ZrV_2, intensify the hydrogen absorbing/desorbing kinetics and electromechanical capacity. However, these binary compounds are too stable in the hydride phase (strong interaction between host metal and hydrogen) and require high temperatures (>250 °C) to release hydrogen [11]. Using X-ray

* *Corresponding author*. Tel./fax: +54 291 4595101x2800.
E-mail address: cajuan@uns.edu.ar (A. Juan).

http://dx.doi.org/10.1016/j.ijhydene.2015.10.077

Please cite this article in press as: Merlino AR, et al., A DFT study of hydrogen storage in $Zr(Cr_{0.5}Ni_{0.5})_2$ Laves phase, International Journal of Hydrogen Energy (2015), http://dx.doi.org/10.1016/j.ijhydene.2015.10.077

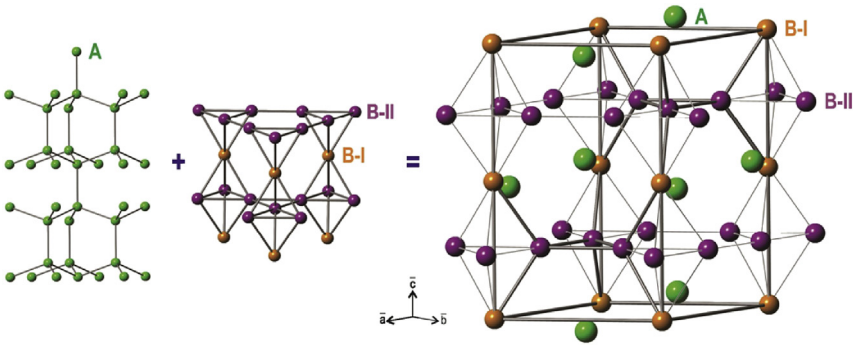

Fig. 1 – A and B atoms nets merged to form the C14 Laves phase. The A sublattice defines a hexagonal diamond net while the B sublattice is only composed of B4 tetrahedra that alternately shares vertices and faces along the c axis. This geometry forms chains of trigonal bypyramids which are linked together by vertex sharing.

diffraction techniques, Yongquan et al. analyzed the crystal structure changes of $Zr(Cr_xNi_{1-x})_2$ ($0.15 \leq x \leq 0.65$) alloy for different Cr concentrations [12]. The authors concluded that the increasing concentrations of Cr intensified the hydrogen storage capacity and that the hydrogen absorption was favored at the larger interstitial cavities.

The open literature present some theoretical research considering hydrogen behavior absorbed in Laves Phases. By semiempirical and ab initio density functional theory (DFT) methods, van Midden et al. studied the structural and electronic properties of the hydrogenated $ZrCr_2$ C14 Laves phase [13]. The authors found that the preferentially occupied sites for hydrogen in the AB_2 matrix were the A_2B_2 tetrahedra. Also by DFT, Gesari et al. investigated the hydrogen absorption in $Zr_{0.9}Ti_{0.1}NiMn_{0.5}Cr_{0.25}V_{0.25}$ C14 alloy and calculated the binding energy for hydrogen at different tetrahedral sites with a variety of local environments [10]. Their results were in agreement with those reported by van Midden et al. [13] In addition, they noted that after hydrogenation there was an increase in the intermetallic volume while the hydrogen binding energy remained almost the same (up to 3.5 hydrogens/formula unit [H/FU]). These facts indicated a small interaction among hydrogen. Matar reported a detailed review of intermetallic hydrides taking into account the contributions of ab-initio calculations to the understanding of chemical bonding and magnetism in binary and ternary Laves phases [14]. Radaković et al. studied the local structural and electronic modifications induced by hydrogen absorption in cubic C15 Laves phases AB_2 (A = Zr; B = Cr, Mn, Ni), as well as the stability of the formed hydrides, by DFT calculations. Their results indicated that a hydrogen distribution within the crystal depended on the level of induced electronic structure modifications [15].

To the best of our knowledge, there is no detailed experimental data available that describe the hydrogen location in a Zr–Cr–Ni Laves phase. In this manuscript, we report a theoretical effort to find the energetically most favorable locations for hydrogen in $Zr(Cr_{0.5}Ni_{0.5})_2$ phase, a C14 type structure where the 50% of Cr atoms were replaced by Ni.

We also analyze the electronic structure of the systems using the density of state (DOS) curves. The changes in the hydrogen absorption energy and magnetic moment are also considered at different H concentrations. Finally, in order to understand the hydride stability we compute the overlap population (OP) values for metal–metal and metal-H bonds.

Crystal structure and intermetallic compound model

Three crystal structures, known as Friauf-Laves phases or more commonly Laves phases, have been observed to

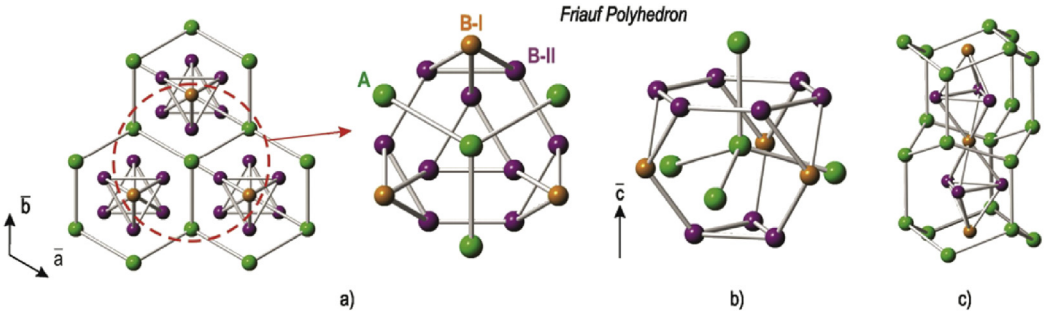

Fig. 2 – Local environment for the C14 system (a). A atoms are surrounded by 16 atoms: 4 A atoms, 3 B-I and 9 B-II (12 B atoms in total). This arrangement is known as the Friauf polyhedron and consists of four B3 triangles linked at their apices to form a truncated tetrahedron with four triangular faces and four hexagonal ones (b).B-I atoms have an environment of 6 A and 6 B-II atoms, while B-II atoms have an environment of 6 A, 2 B-I and 4 B-II atoms (c).

Please cite this article in press as: Merlino AR, et al., A DFT study of hydrogen storage in $Zr(Cr_{0.5}Ni_{0.5})_2$ Laves phase, International Journal of Hydrogen Energy (2015), http://dx.doi.org/10.1016/j.ijhydene.2015.10.077

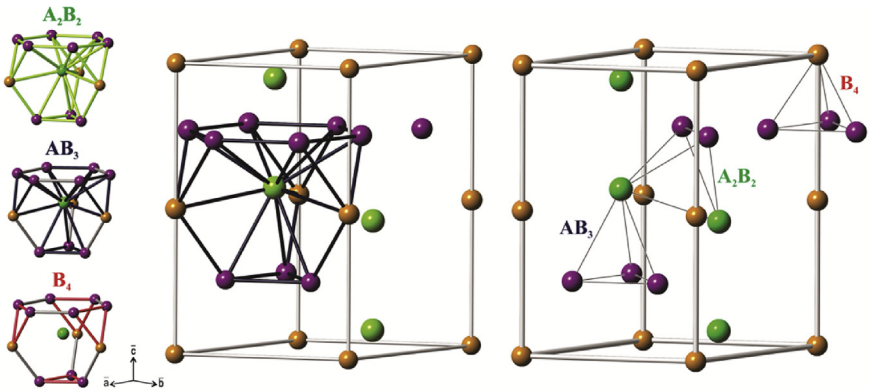

Fig. 3 – Unit cell of the hexagonal $ZrCr_2$ Laves phase with all its possible tetrahedral sites: 12 A_2B_2 sites, 4 AB_3 and 1 B_4.

associate with the ideal stoichiometric AB_2-type intermetallic compounds: cubic $MgCu_2$ (C15) and hexagonal $MgZn_2$ (C14) and less frequently $MgNi_2$ (C36). Generally, the A metal is an electropositive metal, i.e. early transition metal (TM), actinide, alkali metal, alkaline earth or lanthanide; while the B metal is usually a less electropositive TM: Cr, Ni, V, among other metallic elements or even a noble metal. The Laves interstitial sites are tetrahedral and for this reason these structures are all known as tetrahedrally close-packed (TCP) [16–22].

Depending of the synthesis conditions, the $ZrCr_2$ intermetallic can be either a C14 or C15 Lave phase, with four formula units per unit cell [23]. It presents a $P6_3/mmc$ (D^4_{6h}) structure and its lattice parameters are $a = b = 5.221$ Å and $c = 8.567$ Å, where $c/a = (8/3)^{1/2}$. Fig. 1 shows the Zr (A atom) and Cr (B atom) sublattices. The Zr sublattice looks like a hexagonal diamond net, while the B sublattice is composed of B_4 tetrahedra alternatively sharing vertices and faces along the *c* axis, thereby forming chains of apically fused trigonal bipyramids. These chains are linked together by vertex sharing in the *ab* plane. Then the Zr atoms are located in interstitial sites of the Cr sublattice [10].

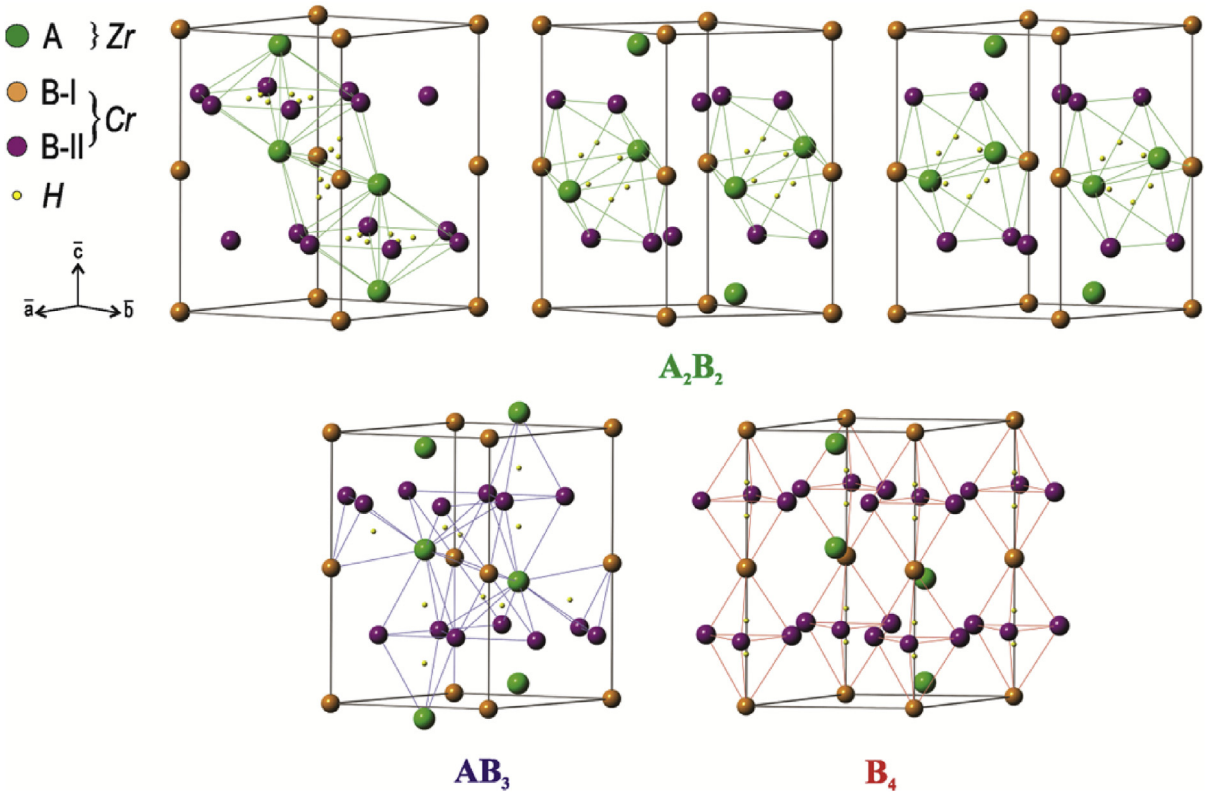

Fig. 4 – All possible sites to locate H in the $ZrCr_2$ structure. Adding the four A-atom neighbors outside the hexagonal faces and other A and B atoms from the net, there are 24 A_2B_2 tetrahedral that has the central A atom as one apex (and that, by symmetry, turn into a total of 42 A_2B_2 sites), 10 AB_3 sites and 16 B_4 distorted icosahedra sites. Hydrogen atoms are represented by small spheres and placed at each interstitial sites.

Please cite this article in press as: Merlino AR, et al., A DFT study of hydrogen storage in $Zr(Cr_{0.5}Ni_{0.5})_2$ Laves phase, International Journal of Hydrogen Energy (2015), http://dx.doi.org/10.1016/j.ijhydene.2015.10.077

Table 1 – Experimental and calculated (this work) lattice parameters, bulk modulus B cell volume and magnetic moment μ for $Zr(Cr_{0.6}Ni_{0.4})_2$ and $Zr(Cr_{0.5}Ni_{0.5})_2$, respectively. Porcentual differences (%) between reported and calculated parameters.

Parameters	$Zr(Cr_{0.6}Ni_{0.4})_2$	$Zr(Cr_{0.5}Ni_{0.5})_2$	%
	Reported	This work	
a (Å)	5.030[a]	5.022	−0.15
c (Å)	8.238[a]	8.241	0.04
c/a	1.6377[a]	1.6409	0.19
B (GPa)[c]	161.5[b,c]	167.17	3.51
Cell volume (Å^3)	180.50[a]	180.04	−0.25
μ (μ_B)	–	1.38	–

[a] Ref. [39].
[b] Ref. [46].
[c] $ZrCr_2$ C15 structure.

Fig. 2 shows the local environment for the C14 system. In this phase, each Zr atom is coordinated with 12 Cr atoms and 4 Zr atoms, leading to the particular configuration known as the Friauf polyhedron [24]. The tetrahedral units are built up from two crystallographic distinct atoms B(I) and B(II), linked by vertex sharing and by triangle B(II)–B(II)–B(II) face sharing. Three different types of tetrahedral sites are available for storing hydrogen. These sites are showed in Fig. 3 and named A_2B_2, AB_3 and B_4. The $ZrCr_2$ structure has 12 A_2B_2 sites per A atom, 4 AB_3 sites and 1 B_4 site per formula unit.

Considering the seven possible independent hydrogen positions per unit cell and multiplying them by their symmetry, then there are 68 possible sites where the H atoms could be located, resulting in $Zr_4Cr_8H_{68}$ formula (Fig. 4).

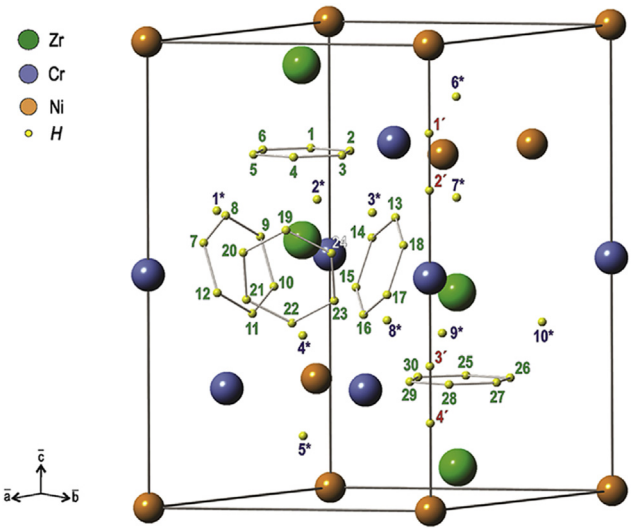

Fig. 5 – $Zr(Cr_{0.5}Ni_{0.5})_2$ unit cell with all possible interstitial sites where hydrogen could be absorbed. Depending on the site, hydrogen atoms are identified by different numbers and colors: A_2B_2 sites are numbered in green color, from 1 to 30; AB_3 sites are numbered in blue color and *, from 1 to 10 and B_4 in red and ′, from 1 to 4. (For interpretation of the references to color in this figure legend, the reader is referred to the web version of this article.)

Despite the important hydrogen storage capacity of this Laves phase, it is not suitable for technological applications due to its strong hydride stability. Previous studies have reported that partial substitutions of Cr by other transition metal, like Ni,

Table 2 – Binding energy (E_B), magnetic moment (μ_B), total cell volume and site volume for $Zr(Cr_{0.5}Ni_{0.5})_2$ with a hydrogen atom placed in each type of interstitial site. Only four most stable sites are described for AB_3 and A_2B_2 interstices.

Tetrahedral site	Site number	Atoms	E_B (eV)	μ (μ_B)	Cell volume (Å^3)	Site volume (Å^3)		
						Before H absorption	After H absorption	ΔV (%)
A_2B_2	29	ZrZrCrCr	−0.28	0.65	180.71	3.20	3.40	6.25
	10	ZrZrCrCr	−0.26	1.81	180.52	3.16	3.24	2.53
	26	ZrZrCrCr	−0.25	0.52	179.37	3.14	3.28	4.46
	17	ZrZrCrCr	−0.20	1.29	183.00	3.16	3.33	5.38
AB_3	9*	ZrCrCrCr	−0.13	1.12	181.66	2.67	2.96	10.86
	5*	ZrCrCrNi	−0.10	1.26	178.98	2.55	2.73	7.06
	4*	ZrCrCrNi	−0.08	1.45	181.60	2.55	2.74	7.45
	6*	ZrCrNiNi	−0.03	1.01	179.87	2.55	2.69	5.49
B_4	3′	CrCrCrNi	0.22	1.36	179.47	No absorption		
	4′	CrCrNiNi	0.26	1.03	180.64			
	1′	CrNiNiNi	0.32	1.64	181.01			
	2′	CrCrNiNi	0.32	0.95	181.30			

The * corresponds to AB_3 sites and ′ corresponds to B_4 sites.

Please cite this article in press as: Merlino AR, et al., A DFT study of hydrogen storage in $Zr(Cr_{0.5}Ni_{0.5})_2$ Laves phase, International Journal of Hydrogen Energy (2015), http://dx.doi.org/10.1016/j.ijhydene.2015.10.077

Table 3 – Bader charges after H absorption in the most stable A_2B_2 (ZrZrCrCr) site (29). Negative signs indicate an increase in the number of electrons. i.e., after H absorption, both Cr atoms increased their negative charge in 0.712 and 0.367, respectively.

Charges after H absorption	Cr	Cr	Zr	Zr	H
	−0.712	−0.367	+2.328	+2.291	−0.960
Δ%	11.87	6.12	58.2	57.28	96.00

could destabilize the hydride [25,26]. These substitutions lead to a constant decrease of the cell volume of the phase due to the small atomic radius of Ni. Nevertheless, its H storage capacity does not change significantly. The hydride can be obtained with a plateau pressure within the range 0.1–1 bar, compatible with electromechanical requirements. According to this, if 50% of Cr is substituted by Ni, resulting in $Zr(Cr_{0.5}Ni_{0.5})_2$, the compound becomes a C14 $MgZn_2$ type structure [27].

The $Zr(Cr_{0.5}Ni_{0.5})_2$ intermetallic was modeled by a hexagonal cell with structural formula $Zr_4Cr_4Ni_4$. H absorption was simulated in the same cell adding a single H atom at each tetrahedral site. Although the substitutions of Cr atoms by Ni were random, we impose the restriction that the cell maintains the Cr/Ni/Zr ratio of 4/4/4. Previous calculations on similar systems indicate no significative changes in energy for this type of substitions [10].

Computational method

We performed first principles calculations based on DFT as implemented in the Vienna Ab-initio Simulation Package (VASP) [28]. This code uses a plane-wave basis set offering good access to the Hellmann–Feynman forces acting on all atoms in the supercell. The projector-augmented wave (PAW) method and spin-polarized DFT with the generalized gradient approximation (GGA) of Perdew, Burke, and Ernzerhof (PBE) were considered [29–33].

The conjugate-gradient (CG) algorithm is used to relax the ions in the Laves phases studied [34]. The convergence in total energy and the force on the atoms were set less than 10^{-4} eV and 10^{-3} eV/Å, respectively. Self-consistent calculations were considered to converge when the difference in the total energy between consecutive steps did not exceed 10^{-4} eV. The k-points were arranged in a standard Gamma centered Monkhorst-Pack grid with a $7 \times 7 \times 5$ mesh [35]. We also tested a $9 \times 9 \times 5$ mesh and no significative improve in energies were found. All calculations were performed using an energy cutoff of 450 eV for the plane wave basis set. The electronic structure and bonding of H– $Zr(Cr_{0.5}Ni_{0.5})_2$ were analyzed by the DOS curves. Bader analysis was used to calculate electronic charges on atoms before and after H absorption [36].

We defined the binding energy (E_B) respect to the isolated molecule as:

$$E_B = [E(AB_2 + nH) - E(AB_2) - E(H_2)\ n/2]/n$$

Table 4 – Binding energy (E_B) per H atom, number of H in unit cell (NH), total energy (E_T), total energy per absorbed H atom (E_T/H), magnetic moment (μ), total cell volume (V) and percentage change in cell volume (ΔV) respect to $Zr(Cr_{0.5}Ni_{0.5})_2$.

Site number	Atoms	E_B (eV)	NH	E_T (eV)	E_T/H (eV)	μ (μ_B)	V (Å^3)	ΔV (%)
29	ZrZrCrCr	−0.28	1	−109.93	−27.48	0.91	191.12	6.15
10	ZrZrCrCr	−0.26	2					
26	ZrZrCrCr	−0.25	3					
17	ZrZrCrCr	−0.20	4					
11	ZrZrCrCr	−0.18	5	−124.31	−15.54	0.75	210.18	16.74
9*	ZrCrCrCr	−0.13	6					
7	ZrZrCrCr	−0.13	7					
28	ZrZrCrNi	−0.12	8					
2	ZrZrCrNi	−0.11	9	−138.31	−11.53	2.86	217.19	20.63
21	ZrZrCrCr	−0.11	10					
24	ZrZrCrNi	−0.10	11					
5*	ZrCrCrNi	−0.10	12					
23	ZrZrCrNi	−0.10	13	−151.80	−9.49	3.17	235.53	30.82
14	ZrZrCrCr	−0.09	14					
18	ZrZrCrNi	−0.08	15					
4*	ZrCrCrNi	−0.08	16					
5	ZrZrCrNi	−0.08	17	−165.64	−8.28	5.37	244.42	35.76
3	ZrZrCrNi	−0.08	18					
9	ZrZrCrNi	−0.07	19					
6	ZrZrCrNi	−0.04	20					
12	ZrZrCrCr	−0.03	21	−178.63	−7.44	5.09	258.97	43.84
15	ZrZrCrNi	−0.03	22					
20	ZrZrCrNi	−0.03	23					
6*	ZrCrNiNi	−0.03	24					
8	ZrZrCrNi	−0.02	25	−189.17	−6.76	4.37	274.00	52.19
27	ZrZrCrNi	−0.01	26					
10*	ZrCrCrNi	−0.01	27					
25	ZrZrCrNi	−0.01	28					

The * corresponds to AB_3 sites.

where $E(AB_2 + nH)$ is the total energy of the AB_2 intermetallic compound containing n H atoms, $E(AB_2)$ is the total energy of the AB_2 without H and $E(H_2)$ is the hydrogen molecule energy [10]. The AB_2 energies, with and without hydrogen, were calculated with the same computational parameters. The third term is the half hydrogen molecule total energy determined by locating a H_2 molecule in a cubic cell of 10 Å sides and carrying out a Γ-point calculation. We obtained a H_2 bond length of 0.751 Å and a binding energy of −4.52 eV in fairly good agreement with experimental values [37]. With this definition, negative absorption energy values correspond to a stable configuration and most likely to be obtaining during experiments [38].

Results and discussion

Lattice parameters were calculated after geometry optimization of the intermetallic structure without H. Table 1 presents experimental ($Zr(Cr_{0.6}Ni_{0.4})_2$) and theoretical ($Zr(Cr_{0.5}Ni_{0.5})_2$) lattice parameters and bulk modulus (**B**). The values obtained are close to the ones reported by Boudina et al. [39] The substitution of Cr by Ni did not originate significant changes in the cell parameters and **B**, in comparison with $ZrCr_2$ laves [40–42]. The **B** value was calculated by fitting the energies from a series

of constant volume relaxations with the Birch–Murnaghan equation of state [43,44]. It was found to be 167.17 GPa, about 6% smaller than values reported by J. Sun et al. [45] and Xing-Qui Chen et al. [9] in their respective ab-initio studies for $ZrCr_2$ Laves phase. Similar results are considered in fairly good agreement with experimental data [41]. Previous studies found that a random distribution of B metals, when substituting Cr by Ni, differs only about 0.1% in the total energy values for different configurations.

To find the hydrogen absorption sites, we first considered the Zr $(Cr_{0.5}Ni_{0.5})_2$ system containing only a H atom in the supercell. As mentioned before, the hexagonal Laves-phase structure has three distinct types of tetrahedral sites suitable for hydrogen occupation (Fig. 3) [47–50]. We carried out total energy calculations for an H atom located at those three different sites (see Fig. 5), each with a different chemical environment, finding that the lowest energies values for hydrogen absorption were mostly located in the A_2B_2 interstitial sites, followed by the AB_3 sites. B_4 sites did not present any favorable locations for H. This means that the filling order is $A_2B_2 > AB_3$, while the B_4 sites will remain empty. Among A_2B_2 sites, the most stable in Zr $(Cr_{0.5}Ni_{0.5})_2$ was the tetrahedral with composition Zr Zr Cr Cr, presenting an H absorption energy value of −0.28 eV (see Table 2). From both chemical and geometrical points of view, atomic hydrogen would prefer the A_2B_2 sites where Zr is present, since it forms a more stable hydride in a very large interstitial site. An isolated hydrogen atom in this type of site is usually in a negative charge state due to charge donation from host elements to hydrogen (see Table 3, Bader Charges). After H absorption, the charge in the most stable A_2B_2 (Zr Zr Cr Cr) interstice reorganize: H and Cr become negatively charged, 96% and 9% respectively, while Zr lose about 58% charge and become positive. The negative charge compels hydrogen to maximize its interatomic distance to the host atoms and, therefore, absorbed hydrogen generally prefers open interstitial sites. The total cell volume changes from 180.04 $Å^3$ to 180.71 $Å^3$ when an H occupies just a single A_2B_2 site, that is an expansion of 0.37%. Considering the volume of the site there is an increase of 6.25% when an H is absorbed at the most favorable A_2B_2 site, other less stable locations present lower volume expansion. In the case of AB_3 sites, with absorption energies of about −0.13 eV/H, the most stable location shows a volume expansion of 10.86%, being lower in other similar sites. Table 5 confirms this expansion showing the elongation of A–A, A–B and B–B distances after H absorption. After hydrogenation,

Table 5 – Hydrogen first neighbor's distances before and after a H atom absorption in the best favorable A_2B_2 and AB_3 sites.

	Site number	Atoms		Zr–Zr	Zr–Cr	Cr–Cr	Zr–Ni	Cr–Ni	Ni–Ni	Zr–H	Cr–H	Ni–H
A_2B_2	29	ZrZrCrCr	–	3.22[a]	3.07[a]	2.65[a]	–	–	–	–	–	–
			H	3.20[b]	3.11[b]	2.80[b]	–	–	–	2.01	1.75	–
	10	ZrZrCrCr	–	3.20	3.07	2.63	–	–	–	–	–	–
			H	3.20	3.08	2.68	–	–	–	2.01	1.72	–
	26	ZrZrCrCr	–	3.22	3.07	2.57	–	–	–	–	–	–
			H	3.20	3.05	2.80	–	–	–	2.00	1.71	–
	17	ZrZrCrCr	–	3.20	3.06	2.63	–	–	–	–	–	–
			H	3.17	3.09	2.82	–	–	–	2.01	1.72	–
AB_3	9*	ZrCrCrCr	–	–	3.07	2.64	–	–	–	–	–	–
			H	–	3.12	2.77	–	–	–	1.98	1.75	–
	5*	ZrCrCrNi	–	–	3.06	2.57	–	2.57	–	–	–	–
			H	–	3.16	2.75	–	2.58	–	1.99	1.74	1.63
	4*	ZrCrCrNi	–	–	3.06	2.57	3.06	2.57	–	–	–	–
			H	–	3.11	2.78	3.10	2.60	–	1.98	1.74	1.61
	6*	ZrCrNiNi	–	–	3.06	–	3.06	2.57	2.57	–	–	–
			H	–	3.30	–	3.03	2.67	2.54	2.04	1.73	1.63

The * corresponds to AB_3 sites.
[a] Before cell relaxation.
[b] After H absorption and cell relaxation.

Table 6 – OP for metal–metal bond with and without hydrogen for the most stable A_2B_2 and AB_3 sites.

Bond	OP					
	29 A_2B_2			9* AB_3		
	Without H	With H	%	Without H	With H	%
Zr–Zr	0.397	0.265	−33.1	–	–	
Zr–Cr	0.184/0.208	0.099/0.119	−46.4/−42.6	0.194/0.210	0.109/0.122	−43.8/−42.0
Cr–Cr	0.166	0.083	−50.0	0.254	0.145	−42.8
Zr–Ni	–	–	–	0.000	0.000	0.000
Cr–Ni	–	–	–	0.106/0.132	0.102/0.127	−4.2/−3.6
Zr–H	–	0.238	–	–	0.258	–
Cr–H	–	0.146/0.151	–	–	0.163/0.164	–
Ni–H	–	–	–	–	0.000	–

The * corresponds to AB_3 sites.

Please cite this article in press as: Merlino AR, et al., A DFT study of hydrogen storage in $Zr(Cr_{0.5}Ni_{0.5})_2$ Laves phase, International Journal of Hydrogen Energy (2015), http://dx.doi.org/10.1016/j.ijhydene.2015.10.077

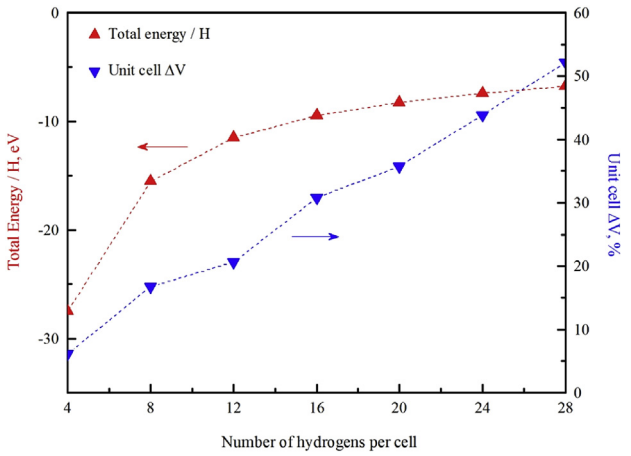

Fig. 6 – Total energy per H and unit cell ΔV (%) vs. number of hydrogen per unit cell in $Zr(Cr_{0.5}Ni_{0.5})_2$ Laves phase.

the computed A–H and B–H distances are slightly longer than those reported in the case of $Zr_{0.9}Ti_{0.1}NiMn_{0.5}Cr_{0.25}V_{0.25}$ [10].

Among A_2B_2 sites, the most favorable sites are Zr Zr Cr Cr and among AB_3 are Zr Cr Cr Cr or Zr Cr Cr Ni. As a preliminary conclusion, tetrahedral with more Ni content destabilizes the hydride. So an increase in the Ni content beyond 50% could be detrimental. In $ZrCr_2$, only the Zr_2Cr_2 site is progressively filled until the formula approaches $ZrCr_2D_{3.5}$, near the experimental limit of absorption, at which point, a minor amount of deuterium may enter $ZrCr_3$ sites [51].

Additionally, we computed the overlap population (OP) between metal–metal atoms before and after H absorption for the most stable A_2B_2 and AB_3 sites. The OP between metal-hydrogen is also calculated. In Table 6 are described these values. For both sites it can be seen that the metal–metal bonds are weakened due to the hydrogen presence. On the other hand the Zr-hydrogen bond is the most important in the metal–H bond. A similar behavior is reported by Porutsky et al. [52].

In order to quantify the H storage capacity, the hydrogen binding energy was computed for different numbers of absorbed H in the system. For each H atom added, a full geometry optimization was carried out, letting the lattice relax. We have found that the binding energy decreases when additional hydrogen concentrations are considered (see Fig. 6). This is an indication of a low interaction among hydrogen atoms in the unit cell. Starting with 4H atoms in the most stable A_2B_2 sites, and then adding successively 4 more H atoms until the system become saturated with 28H atoms per unit cell. The computed cell volume presents a significant change after hydrogenation. Notice an increase of 43.8% in the case of AB_2H_6, that is the cell containing 24H (see Fig. 6). Several authors have reported that after hydrogenation the volume of the AB_2-H_n intermetallic with n between 3 and 4 increases by 15–25% [11,51,53]. Calculations in a related Laves phase predict a volume expansion of about

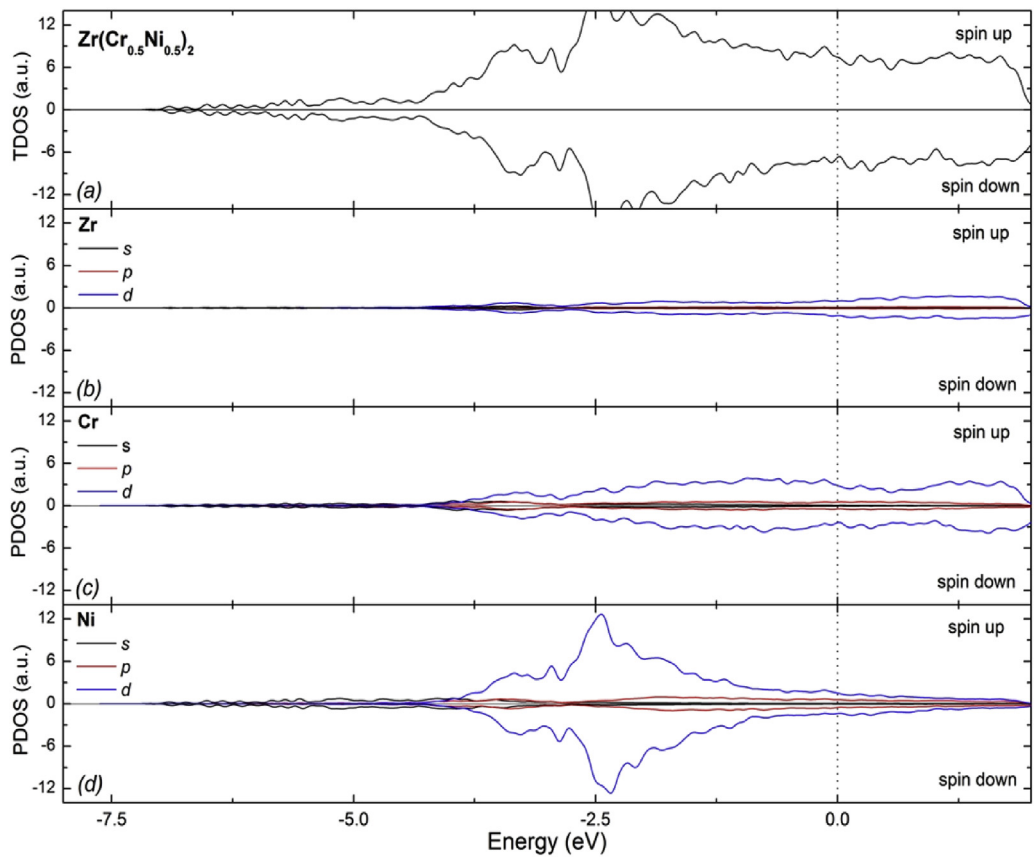

Fig. 7 – Total and projected DOS curves for pure $Zr(Cr_{0.5}Ni_{0.5})_2$. The dotted line indicates the Fermi level.

Please cite this article in press as: Merlino AR, et al., A DFT study of hydrogen storage in $Zr(Cr_{0.5}Ni_{0.5})_2$ Laves phase, International Journal of Hydrogen Energy (2015), http://dx.doi.org/10.1016/j.ijhydene.2015.10.077

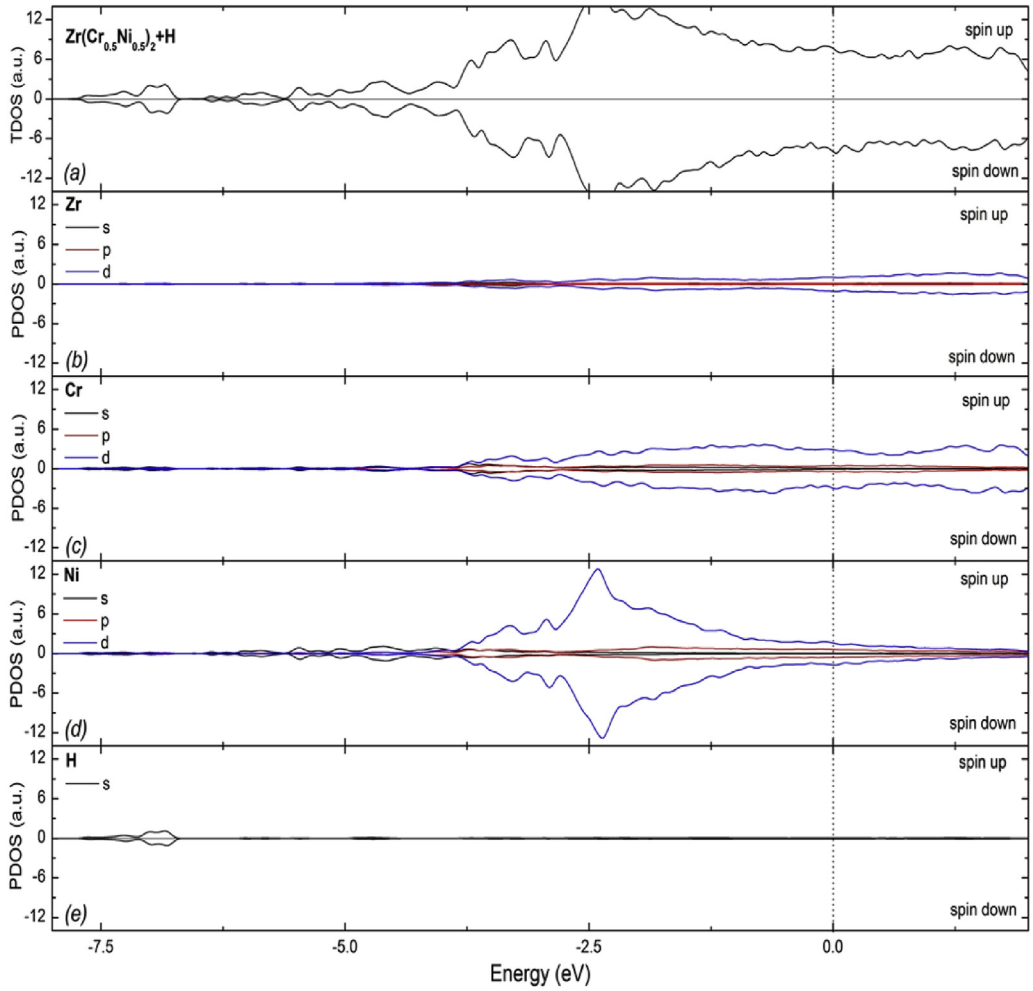

Fig. 8 – Total and projected DOS curves for $Zr(Cr_{0.5}Ni_{0.5})_2$ with a H atom absorbed in the most stable A_2B_2 site. The dotted line indicates the Fermi level.

29% for $AB_2H_{3.5}$ [11]. The computed volume expansion is about 3.2 $Å^3$/H atom which is close to the experimental observed volume expansion, in the order of 2.9 $Å^3$/H atom (10%) [54].

The electronic structure is an important factor in determining the site preference and binding energy of hydrogen to the host system. For this reason the total and projected density of states (DOS) curves of $Zr(Cr_{0.5}Ni_{0.5})_2$ are computed and they are presented in Fig. 7. The total DOS curve for this Laves structure shows that it has a metallic behavior (see Fig. 7a). It can be seen that around the Fermi level this curve is no symmetrical and the magnetic moment obtained is 1.38 μ_B (see Table 1). In addition to this, the $Zr(Cr_{0.5}Ni_{0.5})_2$ total DOS curve around Fermi level has more occupied states respect to $ZrCr_2$ structure [9]. These states are mainly due to Ni *d* electrons (see Fig. 7b to d). From projected DOS (PDOS) curves it can be seen that the principal contribution to the total DOS is due to *d* electrons of all components of the structure. Moreover, the PDOS curves show the *d*–*d* bonding character of $Zr(Cr_{0.5}Ni_{0.5})_2$ as $ZrCr_2$ system [9]. It is well known that a deep valley separates the bonding and antibonding part of the DOS curve and that the stability of the compound depends of the Fermi level location. For $Zr(Cr_{0.5}Ni_{0.5})_2$, the Fermi level is located in the bonging region in comparison with $ZrCr_2$ (see Fig. 7a). Then, $Zr(Cr_{0.5}Ni_{0.5})_2$ structure is more stable that $ZrCr_2$ [55].

Fig. 8 shows the TDOS and PDOS curves for $Zr(Cr_{0.5}Ni_{0.5})_2$ containing one H atom in the A_2B_2 site with composition ZrZrCrCr. There is no noticeable change after hydrogen absorption with respect to pure $Zr(Cr_{0.5}Ni_{0.5})_2$ intermetallic. There are new states between −8 and −7 eV in the TDOS curve due to the H 1*s* states (see Fig. 8e). On the other hand, the absorption of 28H atoms in the structure modified significantly the electronic configuration (see Fig. 9a to e). The introduction of more hydrogen changes the electronic structure of the $Zr(Cr_{0.5}Ni_{0.5})_2$ by the creation of several metal-hydrogen bonding states. The H 1*s* states can be seen in the energy range of −8 to −3 eV (see Fig. 9e). The system remains its conductor behavior. The TDOS and PDOS are no symmetrical and the magnetic computed is 4.38 μ_B. Similar results were reported by Hong et al. in $ZrFe_2$ using DFT calculations [55].

The magnetic moments computed of hydrogenated $Zr(Cr_{0.5}Ni_{0.5})_2$ are listed in Tables 2 and 4 The literature indicate that H absorption has an effect in magnetic properties, and this

Please cite this article in press as: Merlino AR, et al., A DFT study of hydrogen storage in $Zr(Cr_{0.5}Ni_{0.5})_2$ Laves phase, International Journal of Hydrogen Energy (2015), http://dx.doi.org/10.1016/j.ijhydene.2015.10.077

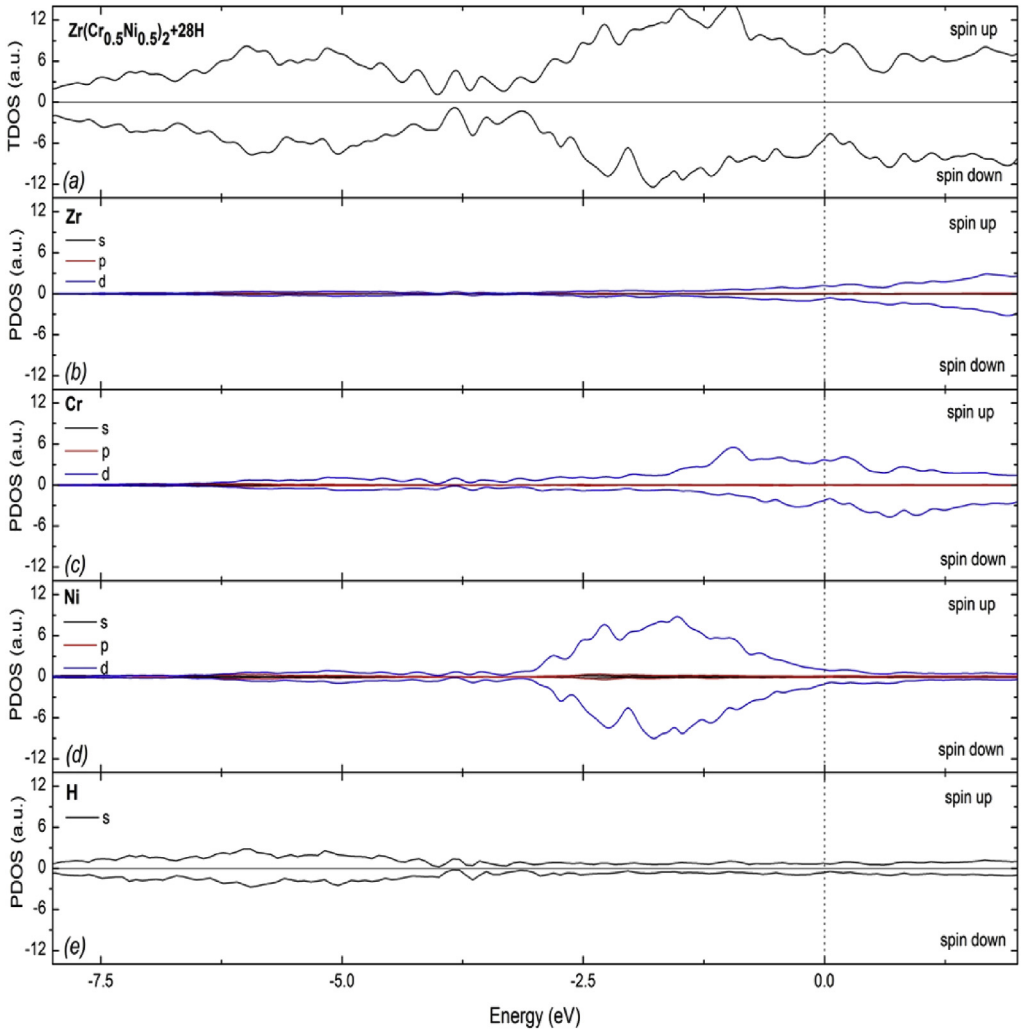

Fig. 9 – Total and projected DOS curves for $Zr(Cr_{0.5}Ni_{0.5})_2$ with 28H atoms absorbed. The dotted line indicates the Fermi level.

effect vary significantly from one host to another [55]. For example, Jacob et al. using X-ray analysis and a vibrating type magnetometer (Stoner type) reported an increase in the susceptibilities, which are directly related to magnetic moment, in $ZrCr_2$ [56]. Hong et al. noted an increase in the magnetic moment with H absorption and they concluded that this fact is partly due to the H-induced lattice expansion [55]. It is clear that above 8H atoms the magnetic moment increase respect to pure $Zr(Cr_{0.5}Ni_{0.5})_2$ Laves phase.

Conclusions

Pure $Zr(Cr_{0.5}Ni_{0.5})_2$ is more stable than $ZrCr_2$ structure, so the replacement of Cr by Ni is a favorable process. Regarding to hydrogen absorption from chemical, electronic and geometrical points of view, atomic hydrogen would prefer A_2B_2 sites with composition Zr Zr Cr Cr. Moreover, an increment of hydrogen amount in this Laves phases leads an increase in the cell volume and magnetic moment $Zr(Cr_{0.5}Ni_{0.5})_2$. We found a lattice expansion of about 52.19% when 28H are absorbed in the unit cell and a saturation energy of −6.76 eV/H. The electronic structure shows bonding interaction dominated by *d*–*d* and *d*-H1*s* states.

Acknowledgments

The authors thankfully acknowledge financial support from the Universidad Nacional de la Patagonia San Juan Bosco, Comodoro Rivadavia, Pcia de Chubut; SGCyT–Universidad Nacional del Sur, CONICET (PIP 20141122013010043 6CO), ANPCyT (PICT 2014–1351, PICT 2012-2186) and CIC–Pcia. de Buenos Aires. Authors would like to specially thank to Dra. P. V. Jasen, Dr. P. Bechthold and Prof. Francisco Bellot Rosado for their valuable contributions. A. Juan, C.R. Luna and M.E. Pronsato are members of CONICET.

REFERENCES

[1] Hansen J, Sato M, Ruedy R, Nazarenko L, Lacis A, Schmidt GA, et al. Efficacy of climate forcings. J Geophys Res 2005;110:D18104.

[2] Schlapbach L, Züttel A. Hydrogen-storage materials for mobile applications. Nature 2001;414:353–8.
[3] Cortright RD, Davda RR, Dumesic JA. Hydrogen from catalytic reforming of biomass-derived hydrocarbons in liquid water. Nature 2002;418:964–7.
[4] Rosi NL, Ekert J, Eddaoudi M, Vodak DT, Kim J, O'Keeffe M, et al. Hydrogen storage in microporous metaleorganic frameworks. Science 2003;300:1127–9.
[5] Shaltiel D, Jacob I, Davidov D. Hydrogen absorption and desorption properties of AB2 Laves-phase pseudobinary compunds. J Less Common Met 1977;53:117–31.
[6] Sakintuna B, Lamari-Darkrim F, Hirscher M. Metal hydride materials for solid hydrogen storage: a review. Int J Hydrogen Energy 2007;32:1121–40.
[7] Züttel A, Hirscher M, Panella B, Yvon K, Orimo S, Bogdanovic B, et al. Hydrogen storage. In: Zuttel A, Borgschulte A, Schlapbach L, editors. Hydrogen as a future energy carrier. Weinheim, Germany: Wiley-VCH; 2008. p. 165–264.
[8] Yamada H. Electronic structure and magnetic properties of the cubic laves phase transition metal compound. Phys B 1988;149:390–402.
[9] Chen XQ, Wolf W, Podloucky R, Rogl P. Ab initio study of ground-state properties of the Laves phase compounds. $TiCr_2$, $ZrCr_2$, and $HfCr_2$. Phys Rev B 2005;71:174101.
[10] Gesari SB, Pronsato ME, Visintin A, Juan A. Hydrogen storage in AB2 Laves phase (A = Zr, Ti; B = Ni, Mn, Cr, V): binding energy and electronic structure. J Phys Chem C 2010;114:16832–6.
[11] Buoudina M, Grant D, Walker G. Review on hydrogen absorbing materials-structure, microstructure and thermodynamics properties. Int J Hydrogen Energy 2006;31:177–82.
[12] Yongquam L, Baran S, Duraj R, Kalychak YM, Przewoźnik J, Szytuła A. The electrochemical charge-discharge properties of Zr–Cr–Ni hydrogen storage alloys. J Alloy Comp 1995;231:573–7.
[13] van Midden HJP, Prodan A, Zupanič E, Žitko R, Makridis SS, Stubos AK. Structural and electronic properties of the hydrogenated $ZrCr_2$ Laves phase. J Phys Chem C 2010;114:4221–7.
[14] Matar SF. Intermetallic hydrides: a review with ab initio aspects. Progr Sol State Chem 2010;38:1–37.
[15] Radaković J, Batalović K, Maarević I, Belošević-Čavor J. Interstitial hydrogen in Laves phases-local electronic structure modifications from first-principles. RSC Adv 2014;4:54769–74.
[16] Villars P, Calvert LD. Pearson's handbook of crystallographic data for intermetallic phases. Materials Park: The Materials Information Society; 1991.
[17] PearsonWB. The crystal chemistry and physics of metals and alloys. New York: Wiley; 1972.
[18] Westbrook JH. Intermetallic compounds. 1st ed. New York: Willey; 1967.
[19] Laves F. Theory of alloy phases. 1st ed. Cleveland:American Society for Metals; 1956.
[20] Friauf JBJ. The crystal structures of two intermetallic compounds. J Am Chem Soc 1927;49:3107–14.
[21] Friauf JB. The crystal structure of magnesium di-zincide. Phys Rev 1927;29:34–40.
[22] Laves F, Witte H. Die kristallstruktur des $MgNi_2$ und seine beziehungen zu den typen des $MgCu_2$ und $MgZn_2$. Metallw 1935;14:645–9.
[23] Chao BS, Young RC, Ovshinky SR, Pawlik DA, Huang B, Im JS, et al. Effect of alloy composition on the structure of Zr-based metal alloys. Mater Res Soc Symp Proc 2000;575:193–8.
[24] Samson S. In: Rich A, Davidson N, editors. Structural chemistry and molecular biology. San Francisco: Feeman; 1968. p. 687.
[25] Pebler A, Gulbransen EA. Thermochemical and structural aspects of the reaction of hydrogen with alloys and intermetallic compounds of zirconium. J Electrochem Tech 1966;4:211–5.
[26] Chartouni D, Züttel A, Nützenadel Ch, Gross K, Schlapbach L, Güther V, et al. Electrochemical properties of Zr $(V_xNi_{1-x})_3$ as electrode material in nickel-metal hydridebatteries. Int J Hydrogen Energy 1999;24:229–33.
[27] Joubert JM, Latroche M, Percheron-Guégan A, Bouet J. Improvement of the electrochemical activity of ZrNiCr Laves phase hydride electrodes by secondary phase precipitation. J Alloy Comp 1996;240:219–28.
[28] Kresse G, Furthmüller J. http://cms.mpi.univie.ac.at/vasp/vasp/vasp.html.
[29] Kresse G, Furthmüller J. Efficient iterative schemes for ab initio total-energy calculations using a plane-wave basis set. Phys Rev B 1996;54:11169.
[30] Kresse G, Furthmüller J. Efficiency of ab-initio total energy calculations for metals and semiconductors using a plane-wave basis set. Comp Mater Sci 1996;6:15–50.
[31] Kresse G, Hafner J. Ab initio molecular dynamics for liquid metals. Phys Rev B 1993;47:558.
[32] Kresse G, Joubert D. From ultrasoft pseudopotentials to the projector augmented-wave method. Phys Rev B 1999;59:1758–75.
[33] Perdew J, Burke K, Ernzerhof M. Generalized gradient approximation made simple. Phys Rev Lett 1996;77:3865–8.
[34] Press WH, Flannery BP, Teukolsky SA, Vetterling WT. Numerical recipies. New York: Cambridge University Press; 1986.
[35] Monkhorst H, Pack T. Special points for brillouin-zone integrations. Phys Rev B 1976;13:5188–92.
[36] Bader RFW. Atoms in molecules – a quantum theory. Oxford: Oxford University Press; 1990.
[37] Huber KP, Hertzberg G. Molecular spectra and molecular structure IV: constants of diatomic molecules. 2nd ed. New York: Van Norstrand Reinhold Company; 1979.
[38] Yakoubi A, Baraka O, Bouhafs B. Structural and electronic properties of the Laves phase based on rare earth type BaM_2 (M = Rh, Pd, Pt). Res Phys 2012;2:58–65.
[39] Bououdina M, Soubeyroux JL, Fruchart D, de Rango R. Structural studies of Laves phases $Zr(Cr_{1-x}Ni_x)_2$ with $0 < x < 0.4$ and their hydrides. J Alloy Compd 1997;257:82–90.
[40] Soubeyroux JL, Bououdina M, Fruchart D, de Rango P. Phase stability and neutron diffraction studies of Laves phases $Zr(Cr_{1-x}M_x)_2$ with M = $(Cu_{0.5}Ni_{0.5})$ and $0 < x < 0.2$ and their hydrides. J Alloy Compd 1995;231:760–5.
[41] Pet'kov VV, Prima SB, Tret'jacenko LA, Kocerzhinskij JA. New information on Laves phases in the Zr-Cr system. Metallofizika 1973;46:80–4.
[42] Suprunenko PA, Markiv VY, Tsvetkova TM. Magnetic and X-ray diffraction study of Laves phases in the ternary systems left brace Ti, Zr, Hf right brace –Cr–Al. Russ Metall 1984;1:207–10.
[43] Birch F. The effect of pressure upon the elastic parameters of isotropic solids, according to Murnaghan's theory of finite strain. J Appl Phys 1938;9:279–88.
[44] Birch F. Finite elastic strain of cubic crystals. Phys Rev 1947;71:809–24.
[45] Sun J, Jiang B. Ab initio calculation of the phase stability, mechanical properties and electronic structure of $ZrCr_2$ Laves phase compounds. Phil Mag 2004;84:3133–44.
[46] Foster K, Hightower JE, Leisure RG. Elastic moduli of the C15 Laves-phase materials TaV_2, $TaV_2H(D)_x$ and $ZrCr_2$. Phil Mag 2000;80:1667–79.
[47] Yvon K, Fischer P. Hydrogen in intermetallic compounds I: electronic, thermodynamic, and crystallographic

Please cite this article in press as: Merlino AR, et al., A DFT study of hydrogen storage in $Zr(Cr_{0.5}Ni_{0.5})_2$ Laves phase, International Journal of Hydrogen Energy (2015), http://dx.doi.org/10.1016/j.ijhydene.2015.10.077

properties, preparation (topics in applied physics). Berlin: Springer; 1988.
[48] Folonari C, Iemmi F, Manfredi F, Rolle A. Metal hydride fuel cells: a feasibility study and perspectives for vehicular applications. J Less Common Met 1980;74:371–8.
[49] Sakai T, Miyamura H, Kuriyama N, Kato A, Oguro K, Ishikawa H. The influence of small amounts of added elements on various anode performance characteristics for $LaNi_{2.5}Co_{2.5}$-based alloys. J Less Common Met 1990;159:127–39.
[50] Fruchart D, Rouaut A, Shoemaker CB, Shoemaker DP. Neutron diffraction studies of the cubic $ZrCr_2D_x$ and ZrV_2D_x (H_x) phases. J Less Common Met 1980;73:363–8.
[51] Mitrokhin SV, Smirnova TN, Somenkov VA, Glazkov VA, Verbetsky VN. Structure of (Ti,Zr)–Mn–V nonstoichiometric Laves phases and $(Ti_{0.9}Zr_{0.1})(Mn_{0.75}V_{0.15}Ti_{0.1})_2D_{2.8}$ deuteride. J Alloys Compd 2003;356:80–3.
[52] Porutsky SQ, Zhurakovsky EA. Soft X-ray emission studies of metal-hydrogen bonding states in zirconium-based laves phase hydrides. J Less Common Met 1986;120:273–80.
[53] Nagasako N, Fukumoto A, Miwa K. First-principles calculations of C14-type Laves phase Ti–Mn hydrides. Phys Rev B 2002;66:155106.
[54] Fukai Y. The metal–hydrogen system: basic bulk properties. 2nd ed. Berlin: Springer; 2005.
[55] Hong S, Fu1 CL. Hydrogen in Laves phase ZrX_2(X = V, Cr, Mn, Fe, Co, Ni) compounds: binding energies and electronic and magnetic structure. Phys Rev B 2002;66:094109.
[56] Jacob I, Davidov D, Shaltiel D. Effect of hydrogen absorption on the magnetic properties of some 3-d Laves phase binary and pseudobinary intermetallics. J Magn Magn Mater 1980;20:226–30.

Please cite this article in press as: Merlino AR, et al., A DFT study of hydrogen storage in $Zr(Cr_{0.5}Ni_{0.5})_2$ Laves phase, International Journal of Hydrogen Energy (2015), http://dx.doi.org/10.1016/j.ijhydene.2015.10.077